

# Optical oxygen sensors move towards colorimetric determination

Xu-dong Wang, Hai-xu Chen, Yun Zhao, Xi Chen, Xiao-ru Wang

**Optical oxygen sensors (OOSs) have extensive applications and have attracted significant attention in recent years. We summarize recent developments involving OOSs, including exploring new oxygen probes, discovery of new supporting materials and novel determination assays. We also provide a development blueprint for oxygen sensing.**

© 2010 Elsevier Ltd. All rights reserved.

*Keywords:* Assay; Colorimetry; Determination; Fluorescence intensity; Fluorescence lifetime; Optical oxygen sensor; Organic dye; Oxygen sensing; Polarization; Supporting material

Xu-dong Wang,

Hai-xu Chen,

Yun Zhao,

Xi Chen\*

Xiao-ru Wang

Department of Chemistry,  
College of Chemistry and  
Chemical Engineering, Xiamen  
University, Xiamen 361005,  
China

Xi Chen

State Key Laboratory of Marine  
Environmental Science, Xiamen  
University, Xiamen 361005,  
China

## 1. Introduction

Oxygen sensors have extensive applications in oceanography, meteorology, biology, and environmental and life sciences, and their design and development present chemists with many challenges.

Because of the deficiencies in the conventional approach to oxygen determination, (e.g., Winkler titration [1]), electrochemical oxygen sensors have been developed rapidly and extensively explored. Various determination methods have emerged and been applied in manufacture, clinical monitoring, medical applications [2–4] and biology [5]. Among electrochemical oxygen sensors, the Clark oxygen electrode [6–8] has been in the mainstream. Currently, Clark oxygen sensors are being miniaturized [2,9] and incorporated into intelligent devices, giving them advantages (e.g., portability, time saving and on-line determination).

Although electrochemical oxygen sensors have extensive applications, they have drawbacks (e.g., short lifetime due to the frequency of purging and changing the electrolyte). The electrolyte needs to be renewed periodically, and that has a negative effect on accuracy and response time. Furthermore, loss of oxygen during the process of determination also affects the performance of Clark oxygen sensors.

Due to these defects in the electrochemical oxygen sensor, a new class of oxygen sensor based on luminescence quenching was constructed and has attracted more attention in recent years. Optical oxygen sensors (OOSs) are expected to be inexpensive, easily miniaturized and simple to use, to have extraordinary sensitivity and reversibility, and not to suffer from electrical interference or oxygen consumption.

The use of OOSs depends on three factors: optical sensing probes; supporting materials; and, determination methods. We review recent developments in OOSs, including exploring new oxygen probes, measurement improvements using dual or multiple probes, discovery of new supporting materials and novel assays for determination.

## 2. Optical sensing probes

### 2.1. Organic dyes

For OOSs, an important mechanism is based on the luminescence quenching of the luminophore in the presence of oxygen, since oxygen is a powerful quencher of the electronically excited state of the luminescent dye molecule. The excited-state lifetime or emission intensity of the luminophore varies with changes in oxygen concentration. Probes available as oxygen sensors are generally classified as luminescent and oxygen-quenchable organic luminescent complexes and luminescent nanomaterials.

*2.1.1. Organic luminescent probes.* Pyrene and its derivatives have relatively long excited-state lifetimes and are efficiently quenched by oxygen, so they have been selected as fluorescence probes for oxygen

\*Corresponding author.

E-mail: xichen@xmu.edu.cn

sensors. Pyrene presents certain advantages as an active luminophore for pressure-sensitive paint (PSP) owing to its pressure sensitivity and low temperature coefficient at ambient temperature [10], but pyrene-based PSPs often lack stability due to the loss of pyrene from the silicon polymer [11].

Replacement of pyrene by pyrene derivatives with lower molecular mobility was therefore considered. Basu et al. (2005) synthesized a new pyrene derivative, 1-decyl-4-(1-pyrenyl) butanoate, which has high oxygen-quenching sensitivity and lower diffusion coefficient in a silicon polymer matrix. Response time, recovery time and film stability were improved [12]. Although pyrene and its derivatives have been successfully used as PSPs in aircraft and wind tunnels, these fluorophores are not viable oxygen probes. They have several disadvantages [e.g., short-wave excitation (330nm), which causes most biomaterials and polymers to display strong background luminescence, and sensitivity is not satisfactory].

Wolfbeis et al [13] used decacyclene in a dual sensor for oxygen and halothane, as the probe could be excited with a blue LED and could successfully overcome the problems caused by pyrene and its derivatives. Decacyclene has been used for years in commercial oxygen sensors and biosensors. It has the advantage of not producing singlet oxygen when quenched.

Besides pyrene and its derivatives, erythrosin B had also been selected as an oxygen indicator. It shows favorable phosphorescence-quenching characteristics related to changes in oxygen concentration [14–16]. Lam et al. [17] reported that the phosphorescence quantum yield of erythrosin B was 2%, and the phosphorescence lifetime was about 0.28 ms [14], which make it quite suitable for oxygen sensing.

Although there have been some applications of these organic luminescent probes in oxygen sensing, the disadvantages (including poor photostability and small Stokes shifts) limit their application.

**2.1.2. Metal-complex organic dyes.** Metal-complex organic dyes have been explored for gas sensing for many years. Due to their strong luminescent intensity and long lifetime, these compounds are widely used as probes for OOSs. Metal-complex organic dyes are classified into two categories:

- the transition metals [e.g., ruthenium (Ru), rhenium (Re), osmium (Os), iridium (Ir), rhodium (Rh) and lanthanide] complexes; and,
- the metalloporphyrins [e.g., platinum (Pt) and palladium (Pd) porphyrin complexes].

Among the luminescent transition-metal complexes, Ru(II) polypyridyl complexes have been used most frequently. The fluorescence of Ru(II) polypyridyl complexes is dominated by the metal-to-ligand charge-transfer process, involving raising an electron from a metal *d* orbit to a ligand  $\pi^*$  orbit. Several derivatives of

the ruthenium complex {e.g., tris(2,2'-bipyridine) Ru(II) ( $[\text{Ru}(\text{bpy})_3]^{2+}$ ), tris(1,10'-phenanthroline) Ru(II) ( $[\text{Ru}(\text{phen})_3]^{2+}$ ), and tris(4,7-diphenyl-1,10-phenanthroline) Ru(II) ( $[\text{Ru}(\text{dpp})_3]^{2+}$ )} have been studied [18–22]. Among the Ru(II) polypyridyl complexes,  $[\text{Ru}(\text{dpp})_3]^{2+}$  shows the best response to oxygen, has a fluorescence lifetime of up to 5.3  $\mu\text{s}$  and a quantum yield of about 0.3 [23]. The response to oxygen using  $[\text{Ru}(\text{dpp})_3]^{2+}$  in a sol-gel matrix has been investigated.

Chen et al. [18] fabricated an oxygen sensor using an organically modified silicate (ormosil) film doped with  $[\text{Ru}(\text{dpp})_3]^{2+}$ , which exhibited a good linear relationship, fast response, long-term stability and enhanced sensitivity to dissolved oxygen.

Recently, McGee et al. [24] designed a nanoporous luminophore  $[\text{Ru}(\text{phen})_3](\text{tfpb})_2$  with a void space in the crystalline lattice where molecular oxygen could freely diffuse in and out. The emission intensity and lifetime quenching of  $[\text{Ru}(\text{phen})_3](\text{tfpb})_2$  displayed strictly linear Stern-Volmer behavior, and a single exponential was observed for the emission-intensity decay for all oxygen concentrations, and that makes the nanoporous luminophore a good oxygen-sensing candidate.

Although Ru(II) polypyridyl complexes have been widely used in oxygen sensing, the sensitivity of Ru(II) complex-based oxygen sensors is still not high enough due to their relatively short lifetimes and the generation of singlet oxygen, which is harmful to organisms that have been quenched, so these drawbacks limit their applications in extremely low-oxygen conditions, especially space exploration.

Luminescent transition metals [e.g., Ru(II), Os(II), Re(I), Rh(III), and Ir(III)] complexes show highly desirable features of long lifetime (100 ns ~ 100  $\mu\text{s}$ ) and high quantum yield, so they show great potential for oxygen sensing [25]. Most transition-metal polypyridine complexes are ionic dyes, and insoluble in organic polymer films, but Ir(III) polypyridine complexes are soluble in those films and display remarkably strong green luminescence with high quantum yield and long lifetime ( $\tau < 2.0 \mu\text{s}$ ). Ir(III) complexes are therefore viewed as novel OOS materials.

Amao et al. [26] developed a highly sensitive OOS based on the luminescence-intensity changes of tris(2-phenylpyridine anion) Ir(III) complex ( $[\text{Ir}(\text{ppy})_3]^{3+}$ ) immobilized in a fluoropolymer.

Recently, Medina-Castillo et al. [27] synthesized a novel phosphorescent Ir(III) complex,  $[\text{Ir}(2\text{-phenylpyridine})_2(4,4'\text{-bis}(2\text{-(4-N,N'-methylhexylaminophenyl)-ethyl)-2-29-bipyridine})\text{Cl}]$  (N-948), as an oxygen probe. N-948 presents a quantum yield greater than 0.50 and a long phosphorescence lifetime (102 ms), which makes this Ir(III) complex a perfect indicator for high-sensitivity oxygen sensing using phosphorescence as the basis for determination.

Mak et al. [28] substituted the ppy ligands of  $[\text{Ir}(\text{ppy})_3]^{3+}$  by ppy-NPh<sub>2</sub> and obtained Ir (ppy-NPh<sub>2</sub>)<sub>3</sub>. The compound exhibits very good solubility in organic solvents and polymers, high phosphorescence quantum yield (70%), long luminescence decay time in the  $\mu\text{s}$  range, which enables easy time-resolved imaging, large Stokes shift that could be excited with a low-cost blue LED and emission easily separated from excitation light.

Ir(ppy-NPh<sub>2</sub>)<sub>3</sub> presents favorable sensing properties for oxygen and could be used for high air-pressure sensing (at least up to 1500 mbar). It should be mentioned that the photostability of iridium complexes is not good enough.

Re(I) complexes, another commonly considered oxygen indicator, generally lack significant absorption beyond 400 nm and their molar extinction values are less than 4000 mol/L/cm around 370–380 nm. By contrast, the typical molar extinctions of Ru(II) complexes are about 15000 mol/L/cm around 450 nm.

Recently, Shen et al. [29] synthesized highly-emissive Re(I) complexes, hydrophobic *cis*-Re(CO)<sub>2</sub>(*c*-dppene)-(dpphen) and water-soluble *cis*-Re(CO)<sub>2</sub>(*c*-dppene)(SO<sub>3</sub>-dpphen) with a negative charge, where *c*-dppene is *cis*-(bis(diphenylphosphino)ethylene, dpphen is 4,7-diphenyl-1,10-phenanthroline, and SO<sub>3</sub>-dpphen is its disulfonate derivative. Compared with their tricarbonyl Re(I) counterparts, these Re(I) complexes show significantly higher molar absorption in the range 350–490 nm, which are similar to those of the Ru(II) polypyridyl complexes. The luminescence lifetimes of these Re(I) complexes are up to 10  $\mu\text{s}$  in oxygen-free solutions.

Os(II) complexes can be excited by low-cost, high-intensity, red diode lasers and applied in the detection of oxygen in living organisms due to their intense red absorption. Amao [30] reviewed the applications of Os(II) complexes in oxygen sensing.

The Rh(III) porphyrin complex and lanthanide complexes [31] have also found application in oxygen sensing [32].

Terbium (III) and europium (III) complexes display markedly strong luminescence with high quantum yield and long lifetime, so OOSs have been developed using them [33–35]. However, the sensitivity of these sensors is relatively low ( $I_0/I < 3$ ).

**2.1.3. Metal porphyrins.** Among all oxygen probes, Pt and Pd porphyrin complexes are the most efficient luminophores, since they present strong luminescence at room temperature, absorb visible light and show large Stokes shifts about 200 nm [36]. Their long excited-state lifetime makes them good candidates for OOS probes [37]. In most cases, the visible absorption of metal porphyrins is caused by  $\pi \rightarrow \pi^*$  transition and the large porphyrin ring. The central metal (e.g., Pt and Pd) facilitates intersystem crossing to the triplet state, which has a significantly longer  $\tau_0$  and enhances oxygen

quenching. Meanwhile, Pt and Pd enhance spin-orbit coupling, so that triplet state  $\tau_0$  is not so long as to be totally quenched by environmental interactions or trace quenchers. As a result, many high-performance OOSs have been developed.

Amao et al. [38] doped PtOEP (OEP is 2,3,7,8,12,13,17,18-octaethyl-21H,23H-porphine) and PdOEP in fluoropolymers and fabricated oxygen sensors. For the PdOEP based sensor, a large  $I_0/I_{100}$  ( $I_0$ : fluorescence intensity at 100% nitrogen;  $I_{100}$ : fluorescence intensity at 100% oxygen) value greater than 188.7 was obtained.

Chu et al. [36] developed two high-performance quenchometric Pt complexes for optical-fiber oxygen sensors, and the  $I_0/I_{100}$  of the [*meso*-tetrakis(pentafluorophenyl)porphyrin] Pt(II) (PtTFPP)-doped and PtOEP-doped oxygen sensors were 68.7 and 82.5, respectively. Furthermore, both sensors yielded linear Stern-Volmer plots.

Huo et al. [39] assembled protonated Pt porphyrins ( $[\text{Pt-8Cn-TPPH}_8]^{8+}$ ) with mesoporous silica MCM-48. The oxygen sensor with  $[\text{Pt-8Cn-TPPH}_8]^{8+}/\text{MCM-48}$  had very high sensitivity ( $I_0/I_{100} > 5000$ ) and rapid response (0.04 s) to the change of oxygen concentration, so as to make a high-performance oxygen sensor. In addition, metalloporphyrin complexes [e.g., platinum meso-tetrakis (4-N-methylpyridyl) porphyrin (PtTMPyP<sup>4+</sup>), platinum meso-tetrakis (4-N-pyridyl) porphyrin (PtTPyP), palladium 5-(4-undecancarboxylpyridyl)-10,15,20-tritylporphyrin (PdPC<sub>10</sub>COOH) and tetrakis(4-carboxyphenyl)porphyrin (TCPP) metal complex (PtTCPP, PdTCPP)] have also been developed for stable, highly sensitive OOSs [40,41].

Due to their large Stokes shift, extinction coefficient, quantum yields, long lifetime, excellent photostability and high luminescence, metal-porphyrin complexes have great potential for high-sensitivity oxygen sensing. Their large Stokes shift could effectively reduce the influence of excitation light. The long lifetime, high quantum yield and extinction coefficient make metal porphyrins perfect oxygen indicators. Thus, oxygen sensors based on metal porphyrins, especially Pt and Pd porphyrin complexes, always possess extraordinary sensitivity and have great potential for applications in extremely low oxygen circumstances.

**2.1.4. Dual emitters.** In general, ratiometric measurement is preferred to the alternative, luminescence measurement, in optical sensors due to, e.g., its proved insensitivity to ambient or scattered light, and instrumental fluctuations. A number of studies have focused on the development of the ratio-based oxygen sensor using dual-emitting dyes that display two largely different emission bands. The first emission possesses a decay time in the ns range, which is insensitive to oxygen pressure (as a “reference” signal); the second emission is

a long-lived highly-sensitive oxygen-quenchable emission.

Kostov et al. [42] first utilized one optical filter and frequency selection of the emission from a new oxygen-sensitive dye [(dppe)Pt{S<sub>2</sub>C<sub>2</sub>(CH<sub>2</sub>CH<sub>2</sub>-N-2-pyridinium)}][BPh<sub>4</sub>] for oxygen-sensing measurement.

More recently, Hochreiner et al. [43] selected metal chelate Al-ferron synthesized by 8-hydroxy-7-iodo-5-quinolinesulphonic acid (ferron) and aluminum as a dual-emission luminescence dye for water-dissolved oxygen sensing, but Al-ferron has the problem of easily bleaching.

Recently, a new type of colorimetric oxygen sensor using a dual emitter was developed. Katoh et al. [44] reported a commercial porphyrin derivative, 5,10,15,20-tetraphenyl-21H, 23H-porphine tetrasulfonic acid, as a sensing probe for colorimetric measurement. In their study, red luminescence was observed under the oxygen-free condition, and the color changed to blue at 5% oxygen. The obvious advantages were that no optical detection system and no data processing were required to make this colorimetric sensor versatile for various rapid, semi-quantitative oxygen measurements.

**2.1.5. Fullerenes.** Fullerene is one of the candidate indicators as an oxygen sensor, and its luminescent characteristics and applications in oxygen sensing have been reviewed [30]. Recently, Nagl et al. [45] introduced an OOS especially suited for sensing oxygen down to the ng/mL range and at elevated temperatures. The method applies E-type delayed fluorescence of the fullerene C<sub>70</sub> in appropriate polymers and can optically sense and image ng/mL levels of oxygen at atmospheric pressure. Table 1 summarizes the luminescent dyes used for oxygen sensors.

## 2.2. Luminescent nanomaterials

Although organic metal-complex dyes have been widely used as sensing probes, some intrinsic disadvantages still exist, including narrow excitation-wavelength range, broad emission profiles, photobleaching, limited Stokes shift, high cost and poor biocompatibility. In the sensing application, fluorescence probes play a key role in understanding the intracellular milieu. Unfortunately, organic dyes cannot be directly used in these situations due to their poor chemical stability, poor photostability, cytotoxicity, and perturbation of the host system. In addition, dispersion of organic dyes throughout the cell results in high backgrounds and low spatial resolution [46].

Several attempts have been made to overcome the above limitations based mostly on encapsulation or immobilization of organic dyes into small, biocompatible sensors. Rosenzweig et al. [47] brought a new approach to chemical sensing. They encapsulated an oxygen-sensitive probe, Ru(phen)<sub>3</sub><sup>2+</sup>, in nm-sized liposomes rather

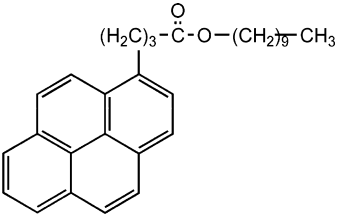
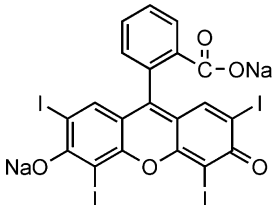
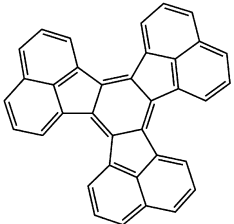
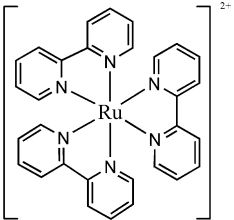
than immobilize the probe into a solid support matrix. The liposomes prepared showed high stability at room temperature and high photostability when they were exposed to excitation light. Individual Ru(phen)<sub>3</sub>-encapsulated liposomes were capable of monitoring an enzymatic reaction with an excellent signal-to-noise ratio (S/N). Their prepared oxygen-sensitive liposomes were used for non-invasive oxygen analysis in tissues and single biological cells.

Kopelman et al. [23] prepared sol-gel probes encapsulated by a biologically localized embedding (PEBBLE) nanosensor through the modified Stöber method. In this approach, Ru(dpp)<sub>3</sub><sup>2+</sup> and Oregon Green 488-dextran, which acts as a fluorescence-intensity reference, were co-immobilized in nanoparticles with diameters of 100–600 nm. The photostable nanosensor presented a reversible response to oxygen for a long period of usage (in excess of 30,000 measurement times). The prepared ratiometric sol-gel PEBBLES were injected into rat C6 glioma cells, and they responded to different oxygen concentrations. The results demonstrated that this approach is feasible and can be extended to provide valuable information about intracellular oxygen.

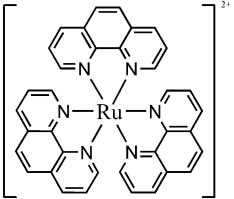
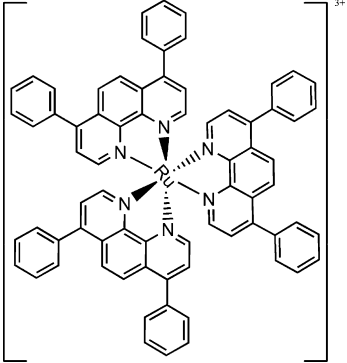
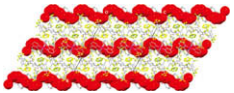
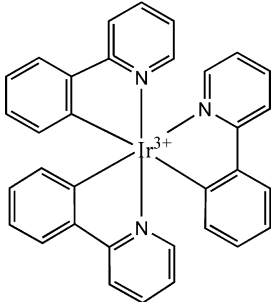
In the same year, Rosenzweig et al. [48] developed μm-sized oxygen-sensitive fluorescent lipobeads for intracellular oxygen measurement. In their research, a high-sensitivity oxygen probe, Ru(bpy-pyr)(bpy)<sub>2</sub>Cl<sub>2</sub> (bpy-pyr = 4-(1''-pyrenyl)-2,2'-bipyridine), was immobilized in a phospholipid membrane coated with polystyrene microparticles. The prepared luminescent lipobeads showed effective quenching behavior to molecular oxygen and prevented direct interaction between probe and cellular macromolecules.

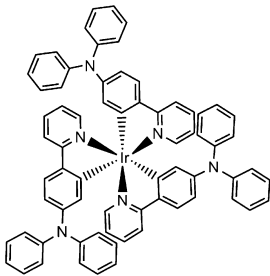
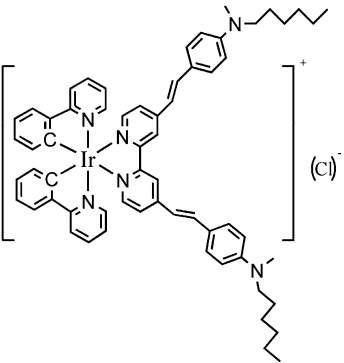
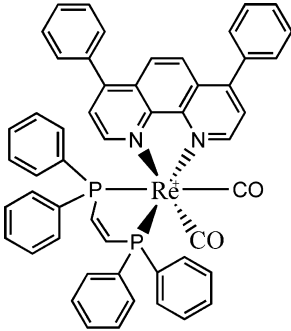
Aspinwall et al. [46] used chemically and environmentally stabilized phospholipid vesicles encapsulating [Ru(phen)<sub>3</sub>]<sup>2+</sup> to construct nanosized, biocompatible oxygen sensors, which showed enhanced stability, wide linear response range, less biofouling and reversible response.

McNeill et al. [49] employed conjugated polymer nanoparticles doped with PtOEP to construct nanosized oxygen sensors for biological imaging. The conjugated polymer nanoparticles possessed an extraordinary light-harvesting ability that could be an excellent energy donor for fluorescence resonance energy transfer (FRET)-based oxygen determinations. Their results revealed that there is highly efficient energy transfer from the conjugated polymer to the metalloporphyrin acceptors, thus resulting in bright phosphorescence, which is very sensitive to oxygen concentration. Single-particle phosphorescence-imaging investigation indicated that the signal from a single particle was sensitive towards partial pressure of oxygen, which generated a great potential for quantitative mapping of local oxygen levels in living cells and tissues.

Probe	Structure	$\lambda_{\text{abs, max}}$ (nm)	$\lambda_{\text{ex, max}}$ (nm)	$\lambda_{\text{em, max}}$ (nm)	Lifetime (s)	Quantum yield	Response time (s)		$I_0/I_{100}$	Support matrix	Ref.
							$\text{N}_2 \rightarrow \text{O}_2$	$\text{O}_2 \rightarrow \text{N}_2$			
DPB		345	300–380	475, 626			10	40		Silicon coatings	[12]
Erythrosin B			532	570, 680	$6.5 \times 10^{-7}$	2%	<1		100	Sol-gel silica	[14]
Decacyclene			385	510				15–20		Silicone rubber	[13]
$[\text{Ru}(\text{bpy})_3]^{2+}$			469	603	$6.5 \times 10^{-7}$	10%	200	300	2.49	Silica–Ni–P composite coating	[21,92]

*(continued on next page)*

Probe	Structure	$\lambda_{\text{abs, max}}$ (nm)	$\lambda_{\text{ex, max}}$ (nm)	$\lambda_{\text{em, max}}$ (nm)	Lifetime (s)	Quantum yield	Response time (s)		$I_0/I_{100}$	Support matrix	Ref.
							$\text{N}_2 \rightarrow \text{O}_2$	$\text{O}_2 \rightarrow \text{N}_2$			
$[\text{Ru}(\text{phen})_3]^{2+}$			480	610	$9.4 \times 10^{-7}$	1.4%				Poly(ethylene glycol) hydrogel	[20,92]
$[\text{Ru}(\text{dpp})_3]^{3+}$			467	592	$5.3 \times 10^{-6}$	30%	30	100	15	DiMe-DMOS Ormosil film	[18,23]
$[\text{Ru}(\text{phen})_3](\text{tfpb})_2$					$6.4 \times 10^{-7}$ ( $\text{N}_2$ ) $1.9 \times 10^{-7}$ ( $\text{O}_2$ )				3.43		[24]
$\text{Ir}(\text{ppy})_3$		376	376	512	$1.5 \times 10^{-6}$ ( $\text{N}_2$ ) $2.5 \times 10^{-8}$ ( $\text{O}_2$ )	90%	4.4	7.3	15.3	Fluoropolymer film	[26]

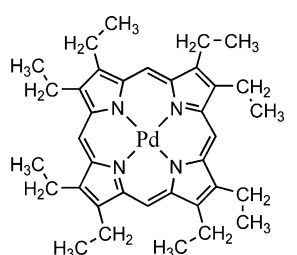
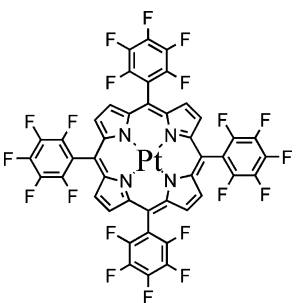
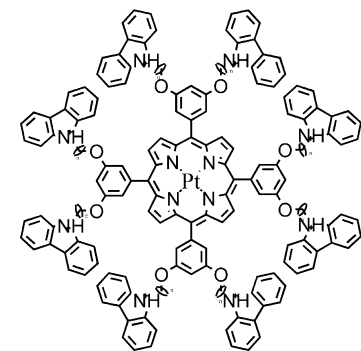
Ir (ppy-NPh <sub>2</sub> ) <sub>3</sub>		405	524	$4.3 \times 10^{-6}$ (N <sub>2</sub> ) $2.5 \times 10^{-8}$ (O <sub>2</sub> )	70%				[28]
N-948		494	665	$1.02 \times 10^{-4}$	58%	10–90 vol% pO <sub>2</sub> <2s	90 to 10 vol% pO <sub>2</sub> <4s	Polystyrene film	[27]
<i>cis</i> -Re(CO) <sub>2</sub> ( <i>c</i> -dppene)(dpphen)		285–290, 380	610	$7.5 \times 10^{-6}$ $-9.3 \times 10^{-6}$	0.3–1.4%				[29]

(continued on next page)

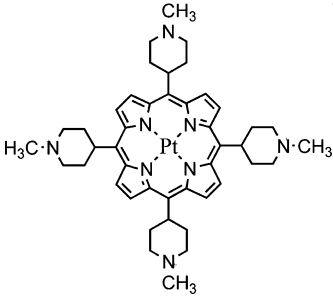
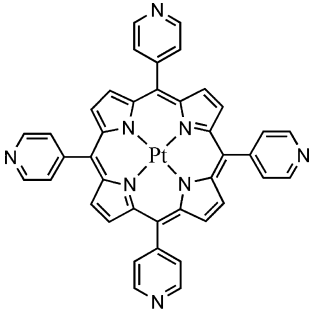
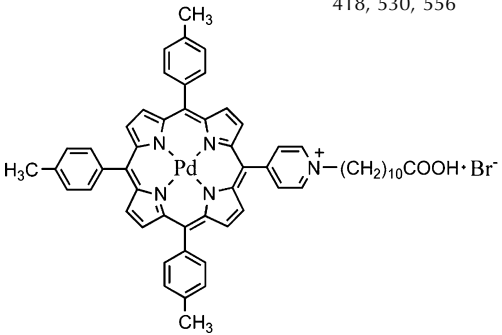
Table 1 (continued)

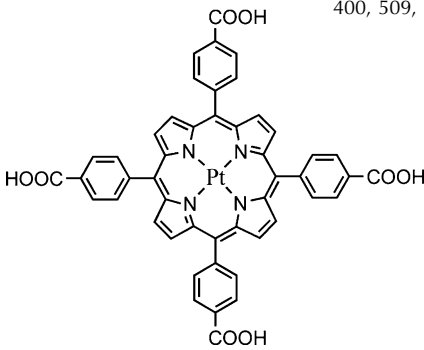
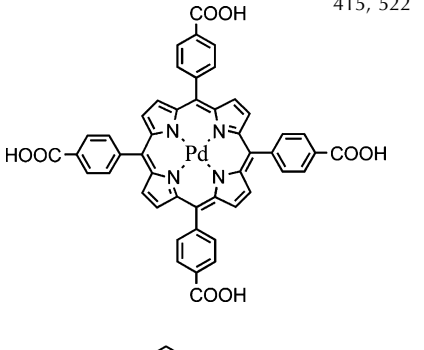
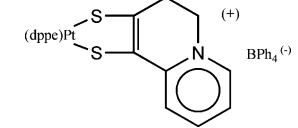
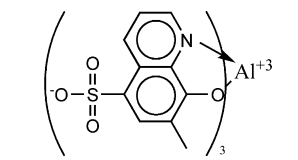
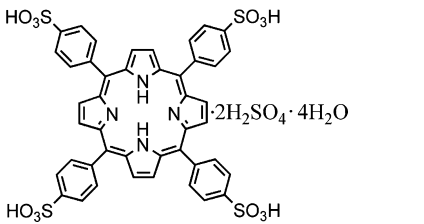
Probe	Structure	$\lambda_{\text{abs, max}}$ (nm)	$\lambda_{\text{ex, max}}$ (nm)	$\lambda_{\text{em, max}}$ (nm)	Lifetime (s)	Quantum yield	Response time (s)		$I_0/I_{100}$	Support matrix	Ref.
							$\text{N}_2 \rightarrow \text{O}_2$	$\text{O}_2 \rightarrow \text{N}_2$			
<i>cis</i> - $\text{Re}(\text{CO})_2(\text{c-dppene})$ ( $\text{SO}_3^-$ - dpphen)		285–290, 380		610	$7.9 \times 10^{-6}$ $-1.05 \times 10^{-5}$	0.3–1.1%					[29]
[Tb(acac) <sub>3</sub> (phen)]		228, 268		490, 546, 590, 620			7.3	70	2.66 (490 nm) 2.68 (546 nm) 2.67 (590 nm) 2.66 (620 nm)	Adsorption film onto alumina plate	[33]
Eu(tta) <sub>3</sub> phen		268, 342	342	612			6.7	7.0	2.40	Poly-(styrene-co- TFEM) film	[35]
PtOEP		384, 500, 535		646	$1.0 \times 10^{-4}$	50%	3.7	5.9	82.5	<i>n</i> -Propyl-TriMOS/ TFP- TriMOS film	[36,116]



PdOEP		394, 512, 546	664	$9.9 \times 10^{-4}$	20%	3	143	682.5	poly-Sty <sub>1</sub> -co-TFEM <sub>2.50</sub> film	[38,116]
PtTFPP		392, 508, 541	650	$6.0 \times 10^{-5}$ (CH <sub>2</sub> Cl <sub>2</sub> )	8.8% (CH <sub>2</sub> Cl <sub>2</sub> )	3.7	5.3	68.7	<i>n</i> -Propyl-TriMOS/ TFP-TriMOS film	[36,117]
[Pt-8Cn-TPPH <sub>8</sub> ] <sup>8+</sup>		404, 510, 540	660		9–11%	0.04	32.2	5041.2	Mesoporous silica	[40]

(continued on next page)

Probe	Structure	$\lambda_{\text{abs, max}}$ (nm)	$\lambda_{\text{ex, max}}$ (nm)	$\lambda_{\text{em, max}}$ (nm)	Lifetime (s)	Quantum yield	Response time (s)		$I_0/I_{100}$	Support matrix	Ref.
							$\text{N}_2 \rightarrow \text{O}_2$	$\text{O}_2 \rightarrow \text{N}_2$			
PtTMPyP <sup>4+</sup>		404, 512, 546		645			<0.5	<30	>50	Mesoporous silica	[40]
PtTPyP				640			<0.75	<221	>7	Mesoporous silica	[41]
PdPC <sub>10</sub> COOH		418, 530, 556		708			26	131	18.3	Alumina plate	[41]

PtTCPP		400, 509, 538	399, 507, 538	665			8.6	50	16.5	Alumina plate	[41]
PdTCPP		415, 522	416, 523	701			36	148	17.7	Alumina plate	[41]
[(dppe)Pt(S <sub>2</sub> C <sub>2</sub> (CH <sub>2</sub> CH <sub>2</sub> -N-2-pyridinium))][BPh <sub>4</sub> ]		440	570 680	3.0 × 10 <sup>-8</sup> (singlet) 2.88 × 10 <sup>-5</sup> (triplet)	0.2% (singlet) 1% (triplet)					Plastic film	[42,92]
Al-Ferron		395	470 580	6.14 × 10 <sup>-7</sup> (470 nm) 6.96 × 10 <sup>-4</sup> (580 nm)						Sol-gel support	[43,98]
5,10,15,20-tetraphenyl-21H, 23H-porphinetetrasulfonic acid		490,650	8.0 × 10 <sup>-9</sup> (N <sub>2</sub> )							Porous alumina film	[44]

The synthesis of luminescent nanocrystals is another way to overcome the above drawbacks of organic dyes. Luminescent nanocrystals, especially quantum dots (QDs), have attracted great attention based on their intensive brightness and good photostability compared with organic dyes. The most intriguing feature of QDs is that their narrow, symmetrical emissions are associated with broad excitations due to quantum confinement. So far, various luminescent nanocrystals have been synthesized [50]. However, only a few of them have reversible responses towards oxygen. Xia et al. [51] report that cadmium telluride (CdTe) QDs capped with 1-cysteine have a size-dependent reversible fluorescence-quenching response towards oxygen. For a QD-based sensor, a distinct and stable emission color change, which is induced by the amount of oxygen and pH of the reaction system, could be obtained by analyte-induced size-dependent quenching of QDs. The results suggested that, based on their unique optical characteristics, QDs would be ideal oxygen probes.

### 2.3. Dual-probe or multiple-probe sensing

Ordinarily, the fluorescence intensity of conventional organic dyes is influenced by the excitation intensity of the light source and ambient temperature, which cause inaccurate fluorescence intensity. A reference signal is helpful to overcome and to correct these effects.

Jorge et al. [52,53] explored an application of semiconductor nanocrystals for an OOS. Due to the great stability of QDs towards photobleaching, they provided a stable reference signal. QDs combined with a ruthenium complex were used to obtain a self-referenced, intensity-based, luminescent oxygen sensor.

The results clearly showed that fluctuation of excitation intensity can be effectively corrected. The oxygen sensor was independent of excitation-intensity fluctuation [52]. Since the emission spectra of QDs can be tailored by composition and size, a suitable reference light can be easily chosen to avoid any spectral overlay. Further more, the luminescence of QDs is temperature dependent, the intensity of QDs correlated with the ruthenium-complex intensity, which could be used to correct the temperature effect of the ruthenium complex while measuring the oxygen concentration.

Besides the temperature-effect correction, dual-probe sensing could also be defined as dual-parameter sensing. Wolfbeis et al. [54] co-immobilized a temperature-sensitive dye ( $[\text{Ru}(\text{phen})_3]^{2+}$ ) and an oxygen probe (fluorinated Pd(II) tetraphenylporphyrin) into poly(styrene-co-acrylonitrile) microparticles for oxygen sensing or poly(acrylonitrile), which is virtually impermeable to oxygen, for temperature sensing. They successfully separated the luminescence of both dyes using either spectrum difference or luminescence-decay time, and achieved simultaneous imaging of oxygen and temperature. The material prepared could be used for contact-

less imaging of pressure and temperature in wind tunnels and would be suitable for biomedical applications due to its biocompatibility.

In general, it is difficult to select suitable multiple organic dyes for multi-analyte sensing due to their fixed excitation wavelengths, which make the synchronous excitation of the dyes difficult. Wolfbeis et al. [55] creatively constructed a dual sensor for simultaneous sensing of temperature and oxygen using a europium (III)  $\beta$ -diketonate complex as the temperature probe and a Pd-porphyrin complex as the oxygen indicator. The main point of their study was that both dyes could be excited by a 405-nm LED and possessed strong brightness. After selection of an appropriate optical filter, two emission signals corresponding to temperature and oxygen concentration could be separated and analyzed. This sensing scheme presents potential applications in medical and biological areas (e.g., high-resolution oxygen profiling and simultaneous imaging of air pressure and temperature in wind tunnels).

Recently, the same group [56] constructed a sensor that could simultaneously determine three parameters (pH, oxygen and temperature). They used a rapid lifetime-determination method and band-pass filters to separate signals from three different indicators and succeeded in avoiding the influence of spectrum overlap. Integrated with a selective material for gas and indirect oxygen determination, the triple sensor could be modified easily into an acidic/basic gas sensor and enzyme-based biosensor, and the temperature sensor would simultaneously correct for effects of temperature.

### 2.4. Prospects

Exploring new fluorescence probes with longer fluorescence lifetime and greater sensitivity towards a variety of oxygen concentrations is the main direction of development for oxygen sensors. With the development of wet chemistry, fluorescent nanoparticles with controllable, unique luminescent properties are becoming a hot spot in this research field. Another mainstream area of research is to apply dual or multiple probes, where the fluorescence probes work together to diminish any negative impacts on sensor performance and to achieve multi-analyte sensing. This kind of research will encourage the development of optical oxygen sensing towards miniature, multi-parameter analysis.

## 3. Supporting materials

Supporting materials play an important role in the fabrication of oxygen sensors. Generally, a good supporting material for probe immobilization should have the following characteristics:

- 1) preparation procedures should be convenient and simple;

- 2) dyes should be firmly encapsulated and difficult to purge from the materials;
- 3) dyes immobilized in the supporting material should keep their photochemical and photophysical properties well; and,
- 4) supporting material should possess a brilliant optical property and decent permeability to oxygen.

Current methods for probe immobilization are classified into three types: absorption; covalent attachment; and, embedding technology. Comparatively, absorption is the easiest method that could be implemented to immobilize diverse reagents.

Amao et al. [57,19] absorbed Pt and Pd porphyrins onto the surface of alumina and obtained a favorable outcome for detecting oxygen in the air and in aqueous solutions. Nevertheless, poor strength between the reagents and the substrates and severe shelling of absorptive reagent restrict its application. The covalent attachment method provides a longer shelf-life than the absorption method. In addition, this approach can avoid aggregation of dyes that have poor solubility in the host matrix, especially when the polarity of dyes is incompatible with the supporting materials.

Winnik and Yam et al. [58,59] immobilized Ru complexes into synthesized polythionylphosphazenes and silicon-dioxide film using the covalent method. Although their sensors exhibited gratifying characteristics, the complicated and time-consuming procedures and the changes in chemical properties caused by the covalent bond decreased the sensing signals.

Compared with the above-mentioned methods, embedding technology for probe immobilization is becoming more attractive due to its excellent characteristics (e.g., versatility, excellent optical properties and less dye leakage). The commonly utilized materials are generally organic or macromolecule substrates [e.g., polyvinylchloride (PVC), polystyrene or Nafion]. Inorganic materials were scarcely involved in probe immobilization until Avnir et al. introduced the sol-gel method [60] to immobilize rhodamine 6G into an organic ceramic. From then on, the sol-gel method gained widespread application in preparing sensing films. Subsequently, the development of hybrid sol-gel materials broadened the domain of sol-gel to play a crucial role in probe immobilization. We summarize below the development and the current applications of organic polymers, sol-gels and ormosil.

### 3.1. Organic polymers

In the past few decades, the application of organic polymers as supporting materials has attracted much interest and developed well in preparing oxygen-sensing films due to their diversity, outstanding characteristics and ease of fabrication [54,61,62]. Amao et al. [30] reviewed these developments.

Generally, a sensing probe is intermingled with a macromolecular organic solution. The mixture is then daubed onto a solid support through a spin-coating process and subsequently forms a thin sensing film, in which the probe maintains a desirable state of uniformity.

Hartmann et al. [63] worked on an Ru(II) complex immobilized in a polystyrene probe and studied its luminescence-quenching behavior. They proposed a reasonable illustration of the non-linear relationship of the Stern-Volmer equation. This non-linearity was attributed to the spatial disorder in the polymer structure that obviously affected the excitation-state property of the probe. In the past few years, diverse organic polymers {e.g., polyethylene, poly(methylmethacrylate), poly(vinylchloride), and typically, fluoropolymer [64]}, have attracted much attention and interest in oxygen-sensor research due to their unique oxygen permeability.

Amao et al. [26] immobilized Ir(ppy)<sub>3</sub><sup>3+</sup> in fluoropolymer films prepared from poly(styrene-co-TFEM). The sensing film showed a more desirable response to oxygen than the conventional polystyrene film, due to the strong, high polarity of the carbon-fluorine bond [65].

There have been many reports on oxygen-sensing research based on fluoropolymers and their derivatives [e.g., fluorinated poly(aryl ether ketone)] [66]. Fluoropolymer films have many brilliant properties that make them suitable for preparing oxygen sensors:

- 1) the whole film has low polarity and strong hydrophobicity, thus permitting oxygen to diffuse readily in and out;
- 2) their high thermal and oxidative stability avoid oxidation and bleaching under sunlight; and,
- 3) their low light absorption eliminates disruption in measurements.

There is no doubt that organic polymers play a crucial role in preparing oxygen sensors, but there are still some drawbacks (e.g., toxicity in preparation, probe leakage and non-biocompatibility). Furthermore, organic polymer films always form with a catenarian structure, which has a negative effect on holding the dyes in the matrix.

### 3.2. Inorganic polymers

Compared with organic polymers, inorganic polymers prepared using the sol-gel method possess many unique advantages:

- 1) sensing films can be fabricated at room temperature, so it is possible to control the composition and most dyes keep their chemical and physical properties;
- 2) their three-dimensional structure is efficient in trapping dyes in the porous substrate and allows the dyes to have more free space to avoid aggregation and collision;
- 3) the ultimate film products are totally inorganic materials, which are environmentally friendly; and,

- 4) it is convenient to obtain desirable products through manipulating preparation parameters (e.g., precursor types and proportion, catalyst, temperature and pH).

Looking back on the history of sol-gel technology for immobilizing a reagent so as to detect a target, the carrier, a ceramic consisting of inorganic oxide, in 1984, Avnir et al. [60] initially generated and used it to embed rhodamine 6G. Apart from being a decent film with optical stability, it was dye stable in the pore, and performed high concentration dye immobilization with admirable dispersive properties and uniformity.

Subsequently, in 1990, Zusman et al. [67] applied the sol-gel technique to preparing a pH sensor and gained ideal results. They compared the pH-sensing dye characteristics in sol-gel and solution, and found that the sol-gel material was a benign carrier to encapsulate the pH dye.

Sol-gel materials had extensive applications in oxygen sensors but, by virtue of the high polarity of the film prepared, many researchers found them to be unsuitable for oxygen diffusion because they resulted in lower quenching sensitivity and the films were fragile and apt to crack, especially in the determination of dissolved oxygen. Naturally, researchers commenced hunting for solutions to this problem [18,68,69].

### 3.3. Hybrid sensing films

Organic polymer films have little resistance to high temperature, even though they have flexibility and favorable gas permeability. On the contrary, sol-gel films resist sunlight and high temperatures but they lack flexibility and crack easily. Hybrid films integrate the advantages of both, and present many special properties [68–70], which broaden the horizons in terms of film preparation for oxygen sensors. The hybrid film applied in oxygen sensing is referred to as an organic-inorganic hybrid film, [18,71,72] and can be classified into two groups – van der Waals force or covalent bond – according to the force between organic and inorganic molecules [73].

The van der Waals force film is the main organic polymer simply with inorganic particles {e.g., silicon oxide, zirconium oxide ( $ZrO_2$ ), and aluminum oxide ( $Al_2O_3$ ) [74–79]}. However, these inorganic particles are not suitable for preparing OOSs based on fluorescence quenching, since most of the metal-oxide matrices are not transparent, except for the silicon-oxide matrix provided by the sol-gel technique [80].

In order to explore more diverse OOSs, more transparent nanostructured metal-oxide matrices have been investigated and developed. The preparation of highly-dispersed metal oxides (e.g.,  $Al_2O_3$ ,  $ZrO_2$ ,  $Fe_2O_3$ ,  $Sb_2O_3$ ) on the surface of cellulose and its derivatives have found numerous applications in recent years [74,76,81]. Based

on numerous references, cellulose is a particularly good polymer to prepare hybrid materials, since it can be molded into different forms (e.g., membranes, spheres and fibers). In addition, novel nanostructured materials (e.g., aluminum oxide), embedded into polyvinylalcohol (PVA) were investigated as potential matrix to incorporate organometallic compounds (OMCs) for the development of OOSs [80,82]. Generally, as Winnik et al. [82,83] stated, addition of the inorganic particles serves three separate functions in the sensing film:

- the inorganic particles are thought to be bound to the particle surface or captured inside porous structures, and then serve as carriers for dye molecules when dyes are poorly soluble in the polymer;
- the inorganic particles serve as a “filler” to reinforce the polymer film and improve its mechanical properties; and, finally,
- the volume fraction of the filler is large enough to hinder coherence of the polymer phase, and yield more void space to increase the surface area and improve the optical properties.

Inorganic hybrid films have received more attention due to their advantages, but the complications resulting from the presence of the inorganic particles in the polymer films have blocked the advanced development of inorganic particle hybrid films.

The covalent-bond film is mainly involved, since a strong covalent bond links inorganic and organic molecules, and this generates coherent, compatible films. Ormosil is such a material in which organic fragments are built into silicon-oxide networks and employed well in preparation and design of oxygen sensors.

Co-hydrolysis results in a mixture of tetraalkoxysilane and alkyl-substituted silicon alkoxides. Due to the non-hydrolyzing alkyl groups structurally acting as a network, many desirable properties have been achieved by these new hybrids for a range of applications.

Schmidt et al. [84] initially produced a series of non-crystal solids comprising organic-modified alkoxy silane and called them ormosil. McDonagh et al. [85] obtained an oxygen-sensor film utilizing methyltriethoxysilane (MTEOS) and ethyltriethoxysilane (ETEOS) or tetraethoxysilane as co-precursors. Klimant et al. [86] had deep insight into the study of ormosil. They prepared  $\mu$ -oxygen-sensing optodes through the sol-gel process using ormosil as the matrix, in which phenyltrimethoxysilane was selected as organic modifier. By comparison, they found that ormosil provided:

- a more desirable environment for the oxygen-sensing dye immobilized in the matrix;
- better oxygen permeability than obtained using MTEOS or ETEOS as organic modifier;
- faster response;
- higher sensitivity; and,
- better linearity of the Stern-Volmer plot.

The utilization of fluorinated ormosil [87,36] was recently developed. Carturan et al. [88] made a detailed study of the fabrication of silicon-oxyfluoride materials with high fluorine contents through the direct hydrolysis of fluoroalkoxide precursors and evaluated the silicon-fluorine bonds within the silicon network. Atkins and co-workers [89] studied the optical properties of highly fluorinated and photosensitive ormosil-derived films for potential use as waveguides.

Subsequently, Pagliaro et al. [87] made an intensive study of  $[\text{Ru}(\text{dpp})_3]^{2+}$  immobilization in the fluorinated xerogels. In their studies, they tailored a sensor platform from a hybrid xerogel-based oxygen sensor comprising n-propyltrimethoxysilane and 3,3,3-trifluoropropylmethoxysilane doped with  $[\text{Ru}(\text{dpp})_3]^{2+}$ , and they found extremely high sensitivity for oxygen. Due to the high hydrophobicity and consequently lower surface tension at the solid/liquid interface during the drying of the intermediate alcogel, crack-free formation was achieved without any added surfactant in preparing the ormosil. The composite ormosil films are smooth and homogeneous. Based on their study results, oxygen sensors fabricated by fluorinated ormosil are more sensitive and stable, and supply rapid detection and a facile approach due to their unique properties.

The desirable advantages of the fluorinated ormosil suggest a prosperous future for their application in oxygen sensors.

### 3.4. Prospects

As mentioned above, the appearance of various new supporting materials improves or removes many drawbacks with conventional OOSs (e.g., dye leakage and being prone to aging). Due to their applications in environmental protection and monitoring, it would be desirable to explore and to utilize advanced supporting materials. Exploring new supporting materials that possess new characteristics would induce future development in such fields. The next generation of supporting materials should have extraordinary advantages, e.g.:

- 1) enhanced selectivity toward oxygen; preventing other substances (e.g., ions and other gases) from entering the film and permitting oxygen only, enhanced selectivity could improve determination accuracy [56];
- 2) in order to attract favorable commercial applications, prolonged shelf-life of supporting materials should be given more attention;
- 3) low or non toxic and environmental-friendly film-preparation methods should be developed; and,
- 4) smooth, transparent, easily miniaturized and integrated sensing films should be explored.

## 4. Methods of determination

There are four basic ways for the optical monitoring of oxygen:

- intensity measurement;
- lifetime measurement, including pulsed luminescence and phase-modulation lifetime methods;
- polarization assay; and,
- colorimetric oxygen determination.

The optical determination of oxygen is always based on the quenching behavior of the sensing probes that obey the rules of the Stern-Volmer equation, which quantitatively relates lifetime and luminescence intensity to oxygen concentration:

$$\frac{I_0}{I} = \frac{\tau_0}{\tau} = 1 + K_{sv}[O_2] \quad (1)$$

where:  $K_{sv}$  is the Stern-Volmer quenching constant;  $\tau$  and  $\tau_0$  are quenched and unquenched fluorescence lifetimes, respectively; and,  $I$  and  $I_0$  are quenched and unquenched fluorescence intensities, respectively. The response of an ideal sensor based on Stern-Volmer quenching kinetics has a linear relationship with oxygen concentration. From the Stern-Volmer equation, it is easily observed that quantitative measurement of oxygen can be based on fluorescence intensity or lifetime.

### 4.1. Fluorescence intensity

The determination of oxygen based on fluorescence intensity is the simplest method, and is still a very common in fluorometry, by which oxygen concentration is calculated according to the Stern-Volmer equation. The advantages of fluorescence-intensity-based oxygen determination include simplicity and low cost. The major disadvantage is that the emission intensity is strongly affected by the stability of the light source, variations in the efficiency of the transmission optics, detector sensitivity, photodecomposition of probes and inhomogeneous dye distribution [90]. Light-source and transmission-intensity fluctuations could be corrected using a double-beam assay [91], dual emitter [92,42] or reference scatterer. Photodecomposition is an unpredictable factor of signal loss; it could be avoided effectively by using photochemically-stable probes and reducing light exposure by decreasing the intensity or the duty cycle. In order to overcome these practical drawbacks, ratiometric measurement was developed [92,93].

### 4.2. Fluorescence lifetime

Fluorescence lifetime is an intrinsically important parameter of a fluorophore, since it determines the time available for the fluorophore to interact with or diffuse in its environment. The fluorescence lifetime reflects information about the ambient conditions of the fluorophore. Since fluorescence lifetime is independent of the perturbation of excitation intensity, detector sensi-

tivity and drift, geometry changes, photodecomposition [94] and, most importantly, indicator concentration, its measurement could effectively avoid the influence of external factors and obtain accurate, irreplaceable data that could not be obtained by fluorescence-intensity-based determination. However, fluorescence-lifetime measurement needs sophisticated, expensive instruments and is unsuitable for practical applications. However, with the advent of luminophores whose lifetimes range from hundreds of ns to hundreds of  $\mu$ s, lifetime sensing was no longer restricted to ultra-short lifetimes [95].

So far, there are two common methods of measuring the fluorescence lifetime: time domain (always referred to as pulse fluorometry); and, frequency domain (phase-modulation fluorometry).

**4.2.1. Pulse fluorometry.** In pulsed-lifetime measurements, a pulse of light, which is made as short as possible and is preferably much shorter than decay time  $\tau$  of a sample, is needed to excite the sample. Single-exponential decay is ideal and favored in pulsed-lifetime measurements, but multi-exponential decays, which increase data-processing complications severely, are always obtained. The rapid lifetime-determination method is a good option to deal with single-exponential and double-exponential decays [96] and can handle even multi-exponential decays. However, this method could not deal with short-lived fluorescence-based determination. To overcome this drawback, Klimant et al. [97] introduced the time-domain dual-lifetime reference (td-DLR) method. They employed two luminophores with different lifetimes, with at least one lifetime in the  $\mu$ s range. The short-lived indicator and the long-lived inert reference dye are simultaneously excited and measured in two time gates. The first ( $A_{\text{ex}}$ ) is in the excitation period in which the light source is on and the signal obtained comprises short-lived fluorescence and long-lived luminescence. The second gate ( $A_{\text{em}}$ ) is opened in the emission period in which the intensity exclusively comprises the reference luminescence. The rise and the decay of the short-lived indicator fluorescence is excluded from the measurement using a delay. Ratioing both images results in an intrinsically-referenced signal that is not affected by the usual optical interferences. This enables the measurement of short-lived lifetime-based optical sensing using simple devices.

Fluorescence-lifetime standards are extremely useful in testing and calibration of metal complexes with long-lived excited-state-sensing systems, but there is a practical need for standards that are applicable over a wide range of temperatures and oxygen pressures.

Morris et al. [94] developed a method to achieve rapid, efficient determination of excited lifetimes, which depends on the temperature and the oxygen concentration in a variety of systems. The method was used to

characterize two systems,  $[\text{Ru}(\text{dpp})_3]\text{Cl}_2$  and  $[\text{Ru}(\text{bpy})_3]\text{Cl}_2$ , in different solvents, and each system can be used as a lifetime standard. This approach permits laboratory and extensive field calibration of instruments and enhanced precision of time-domain lifetime measurements.

**4.2.2. Phase modulation.** For fluorescence probes with a long lifetime, the phase-modulation method is preferred because the long decay time loses significant fractions of the total emission. This loss becomes critical in the presence of a quencher and leads to relatively low S/Ns. Moreover, pulsed-lifetime measurements involve very expensive, complex instrumentation when the fluorescence lifetimes are in the ns range or below.

Compared with pulsed fluorometry, the phase-modulation method offers several advantages:

- 1) S/N can be significantly increased simply by choosing a specific frequency;
- 2) the corresponding lifetime can be calculated through phase shift or amplitude changes; and,
- 3) there are fewer effects from scattered or background light than in pulsed fluorometry [98].

Generally, the phase-modulation method applies a sinusoidally-modulated excitation-light source rather than a pulsed source. There is a phase shift,  $\phi$ , between excitation and emission, which is given by:

$$\phi = \arctan(\omega\tau_\phi); \quad \omega = 2\pi f \quad (2)$$

where  $f$  is the modulation frequency. Phase shifts are easy to measure precisely, and the equipment can be inexpensive. The primary disadvantage of phase-shift instruments is that they generally provide only a single phase shift at one frequency, and lifetime still needs to be calculated [94].

Ogurtsov et al. [99] considered that instrument noise depends on the modulation frequency of excitation, especially in practical sensing devices. They systematically investigated the contribution of noise characteristics using model experiments with an oxygen-sensing film immobilizing Pt(II) porphyrin-ketone complex and polystyrene. They found that the optimal working frequency may significantly differ from the theoretical frequency. With the optimal working frequency, the performance of practical OOSs improved and accurate results could be obtained.

Trettnak et al. [100] constructed a cheap, simple oxygen-determination system based on phase-shift lifetime measurement, in which a Pt(II) porphyrin-ketone complex was employed as the oxygen-sensing probe. The decay time was indirectly obtained by measuring the phase shift between a square-wave excitation and a square-wave in the detector at a single frequency. The frequency proved suitable for oxygen measurement in



both gases and liquids. This system did not need to modulate the high frequency so that it simplified tremendously the phase-modulation-determination method.

Rao et al. made important steps towards the ratiometric oxygen-sensing approach by effectively reducing the influence of light-source fluctuation using the phase-modulation method [92,42,98,101]. Fluorescent dye dppe-Pt2P was employed for oxygen detection based on modulating the fluorescence at two different frequencies. The output signal, which was independent of frequency fluctuation, was obtained by choosing frequencies in the modulation plateaus. More accurate determination of modulation amplitudes and increased S/N could be achieved by using lock-in techniques [42]. Different determination methods (e.g., wavelength ratiometry, lifetime discrimination and polarization detection) were compared. The sensor responses showed significant non-linearity when wavelength ratiometry and polarization methods were applied. A linear Stern-Volmer plot could be obtained, using the frequency discrimination of the lifetime of a dual emitter, which showed particular advantages compared with other assays [92].

Campo et al. [98] introduced a “ratiometric dual phase-shift” method and employed dual-emitter Al-Fer-ron, which presented oxygen-dependent phosphorescent emission and oxygen-independent fluorescent emission, to test this method. Their method can be employed for chemical sensing, even when both lifetimes of the luminescent emissions (reference and indicator) change in the presence of the analyte. Only a different lifetime is necessary in the sensing application. The analytical performance, linear range and limits of detection (LODs) improved remarkably.

The same group compared the frequency-domain-ratiometric method and the wavelength-ratiometric method for optical luminescence sensing. They found that the choice of methodology depended mainly on the spectral and the dynamic response of the indicator used. The frequency-domain-ratiometric method adapted to active phases comprising luminophores that exhibit dual emissions with different lifetimes. However, the wavelength-ratiometric method is more suitable for fluorescence-intensity sensors [102].

### 4.3. Polarization

Although fluorescence-intensity and fluorescence-lifetime methods have been well explored, the theory of these assays is based on a dilute solution, and they cannot be used in concentrated solutions or solutions with high viscosity. Anisotropy-based determination can successfully deal with systems with high viscosity (e.g., cell sap containing large numbers of organelles) and can provide information on the size and the shape of proteins or the rigidity of various molecular environments [103].

The polarization method is simple and accurate, and does not require sophisticated instruments or professional operators.

Anisotropy is another fundamental property of fluorescence emission. Its measurement is based on the photoselective excitation of fluorophores by polarized light. Only those fluorophore molecules whose absorption-transition dipole is parallel to the electric vector of the excitation can be selectively excited. Measured anisotropy  $r$  obeys the Perrin equation:

$$r_0/r = 1 + \tau/\theta \quad (3)$$

where  $r_0$  is the initial anisotropy in the absence of rotation,  $r$  is the measured anisotropy,  $\tau$  is the fluorescence lifetime, and  $\theta$  is the rotational correlation time.

Fluorescence anisotropy  $r$  is measured from the fluorescence intensities observed through polarizers oriented parallel ( $I_{\parallel}$ ) and perpendicular ( $I_{\perp}$ ) to the polarization of the excitation light, which is quite complicated. Rao et al. [104] investigated the fluorescence polarization of a dual emitter with largely different lifetimes and made a simple approach to anisotropy measurement.

$$r = \frac{I_{\parallel} - I_{\perp}}{I_{\parallel} + 2I_{\perp}} \quad (4)$$

$$r = \frac{I_1}{I_1 + I_2} r_1 + \frac{I_2}{I_1 + I_2} r_2 \quad (5)$$

Theoretically, if two emitting species present different steady-state intensities  $I_1$  and  $I_2$ , observed anisotropy  $r$  could be calculated from Equation (5), where  $r_1$  and  $r_2$  are the anisotropies.

$$r = \frac{I_L}{I_L + I_S} r_L + \frac{I_S}{I_L + I_S} r_S$$

$$\frac{r_{OL}}{r_L} = 1 + \frac{\tau_L}{\theta}, \text{ when } \tau_L \gg \theta, r_L \approx 0$$

$$\frac{r_{OS}}{r_S} = 1 + \frac{\tau_S}{\theta}, \text{ when } \tau_S \ll \theta, r_S \approx r_{OS} \quad (6)$$

$$r = \frac{I_S}{I_L + I_S} r_S = \frac{1}{\frac{I_L}{I_S} + 1} r_S = \frac{1}{n + 1} r_S \quad \left( n = \frac{I_L}{I_S} \right)$$

Assume a fluorophore with two emissions of significantly different lifetimes:  $\tau_s$  is significantly shorter than  $\theta$  and  $\tau_L$  is significantly longer. Equation (6) can be derived from the Perrin equation and Equation (5), from which it can be found that any change of the intensity of the long lifetime will result in the change of observed anisotropy  $r$ .

$$\frac{I_{L0}}{I_L} = 1 + k_{SV}[O_2] \quad (7)$$

$$r = \frac{r_S}{\frac{n_0}{1+k_{SV}[O_2]} + 1} \quad (8)$$

In the investigation of Rao et al. [92], the long-lifetime intensity depended only on the oxygen concentration,

which obeys the rule of Stern-Volmer Equation (7). Combination of Equations (6) and (7) gives Equation (8), which means that the oxygen concentration could be obtained from measuring anisotropy  $r$ , where  $n_0$  is the ratio of the long-lifetime and short-lifetime intensities in the absence of  $O_2$ .

Based on the above principle, Rao et al. [104] constructed a novel oxygen-polarization sensor using a dual-emitter molecule that changed the observed anisotropy of its emission as the oxygen concentration varied. It was an important approach to probing in viscous media (i.e. cell protoplasm) and developing polarization-based sensors.

#### 4.4. Colorimetry

So far, many oxygen sensors based on pressure, electrochemistry and photochemistry have been made for accurate quantitative determinations [29,105–109], but these require large scientific instruments with complicated data-collecting and processing systems, so increased costs and the requirement for a professional operator severely limit their usage.

Since Evans et al. [110–112] first reported a novel luminescence-based colorimetric oxygen sensor with a “traffic light” response, a new approach has become available for colorimetric oxygen determination without any assisting instruments. They employed dual (or triple) fluorophores with different oxygen sensitivities and successfully changed emission color. Due to complete or partial fluorescence quenching of one or all of the sensing elements in the sensor, the color change was found to be from red to green at different oxygen concentrations. The sensor did not present well one-to-one apparent-color corresponding to various concentrations of oxygen, since all the fluorophores employed had quenching behavior towards oxygen. The color response of colorimetric luminescent oxygen sensors was therefore described in terms of Commission Internationale de l’Éclairage (CIE)  $x$ ,  $y$  color coordinates. Since then, there have been few, if any, attempts to fabricate a colorimetric oxygen sensor [113].

Although these research groups made important steps towards the colorimetric oxygen determination, several disadvantages still exist (e.g., low resolution, high cost, lack of simultaneous excitation at a single wavelength, and, failure fully to achieve different color changes for different uses).

In order to achieve colorimetric oxygen determination with precise, distinct and tunable color, Wang et al. [114] constructed an OOS strip based on CdTe QDs and [*meso*-tetrakis(pentafluorophenyl) porphyrinato]Pt(II) (PtTFPP). In their sensor strip:

- the QDs are stable to oxygen due to the passive shell;
- the selected fluorescence quenching probe, PtTFPP, presents a good linear response towards oxygen concentration; and,

- PtTFPP provides a one-to-one corresponding relationship between apparent color and oxygen concentration.

After this configuration, accurate oxygen concentration can be simply measured by apparent color, and no data processing is necessary. Based on the principle that they have described, various types of gas, temperature, pH, or ion sensor could be developed by simply replacing the oxygen-sensing probe with other sensing elements.

It is very important that the apparent color can easily be tuned for different uses, especially in multi-analyte determination using the array method. Because of the size-tunable emission character of QDs, the reference color can be changed easily by tuning the size of the nanoparticles. This allows different analyte-sensing units to have distinct colors and generates potential applications for high-throughput analysis. In addition, the use of QDs as the reference signal can efficiently reduce the effect of light-source fluctuation, and allow calibration of the temperature effect [115]. However, the potential cytotoxicity of QDs should be taken into consideration.

#### 4.5. Prospects

Colorimetric oxygen determination has received much attention in recent years due to its simplicity and convenience, and it should become widely used. With improvements in the resolution and the LOD of the colorimetric method, a simplified, accurate, high-resolution method for oxygen determination will enter the mainstream.

#### Acknowledgements

This research work was financially supported by the National Nature Scientific Foundation of China (NSFC, No. 20775064, No. 20975085), Key Project of NSFC (20735002) and the National Basic Research Program of China (2010CB732402), which are gratefully acknowledged. Professor John Hodgkiss is thanked for polishing the English.

#### References

- [1] L.W. Winkler, Ber. Deutsch. Chem. Gos. 21 (1888) 2843.
- [2] M. Dilhan, D. Estève, A.M. Gué, O. Mauvais, L. Mercier, Sens. Actuators, B 26–27 (1995) 401.
- [3] S. Iguchi, K. Mitsubayashi, T. Uehara, M. Ogawa, Sens. Actuators, B 108 (2005) 733.
- [4] M.T. Makale, J.T. Lin, R.E. Calou, A.G. Tsai, P.C. Chen, D.A. Gough, Am. J. Physiol. Heart Circ. Physiol. 284 (2003) 2288.
- [5] M.A. Hanson, X. Ge, Y. Kostov, K.A. Brorson, A.R. Moreira, G. Rao, Biotechnol. Bioeng. 97 (2007) 833.
- [6] M. Wittkamp, G.C. Chemnitz, K. Cammann, M. Rospert, W. Mokwa, Sens. Actuators, B 43 (1997) 40.
- [7] R.S. Luz, F.S. Damos, A.A. Tanaka, L.T. Kubota, Sens. Actuators, B 114 (2006) 1019.

- [8] Y. Hu, O.K. Tan, J.S. Pan, X. Yao, *J. Phys. Chem. B* 108 (2004) 11214.
- [9] M.S. Lin, H.J. Leu, C.H. Lai, *Anal. Chim. Acta* 561 (2006) 164.
- [10] Y. Mébarki, *Pressure Sensitive Paints: Application in Wind Tunnels*, ONERA NT 1998-6, PhD Thesis, University of Lille, France, 1998, pp. 1–143.
- [11] B.J. Basu, C. Anandan, K.S. Rajam, *Sens. Actuators, B* 94 (2003) 257.
- [12] B.J. Basu, A. Thirumurugan, A.R. Dinesh, C. Anandan, K.S. Rajam, *Sens. Actuators, B* 104 (2005) 15.
- [13] O.S. Wolfbeis, H.E. Posch, *Anal. Chem.* 57 (1985) 2556.
- [14] M.A. Chan, J.L. Lawless, S.K. Lam, D. Lo, *Anal. Chim. Acta* 408 (2000) 33.
- [15] R.T. Bailey, F.R. Cruickshank, G. Deans, R.N. Gillanders, M.C. Tedford, *Anal. Chim. Acta* 487 (2003) 101.
- [16] R.N. Gillanders, M.C. Tedford, P.J. Crilly, R.T. Bailey, *J. Photochem. Photobiol., A* 162 (2004) 531.
- [17] S.K. Lam, E. Namdas, D. Lo, *J. Photochem. Photobiol., A* 118 (1998) 25.
- [18] X. Chen, Z. Zhong, Z. Li, Y. Jiang, X. Wang, K.Y. Wong, *Sens. Actuators, B* 87 (2002) 233.
- [19] Y. Amao, I. Okura, *Sens. Actuators, B* 88 (2003) 162.
- [20] D.P. O'Neal, M.A. Meledeo, J.R. Davis, B.L. Ibey, V.A. Gant, M.V. Pishko, G.L. Coté, *IEEE Sens. J.* 4 (2004) 728.
- [21] X. Xiong, D. Xiao, M.M.F. Choi, *Sens. Actuators, B* 117 (2006) 172.
- [22] L. Guo, Q. Ni, J. Li, L. Zhang, X. Lin, Z. Xie, G. Chen, *Talanta* 74 (2008) 1032.
- [23] H. Xu, J.W. Aylott, R. Kopelman, T.J. Miller, M.A. Philbert, *Anal. Chem.* 73 (2001) 4124.
- [24] K.A. McGee, D.J. Veltkamp, B.J. Marquardt, K.R. Mann, *J. Am. Chem. Soc.* 129 (2007) 15092.
- [25] K.A. Kneas, W. Xu, J.N. Demas, B.A. DeGraff, A.P. Zipp, *J. Fluoresc.* 8 (1998) 295.
- [26] Y. Amao, Y. Ishikawa, I. Okura, *Anal. Chim. Acta* 445 (2001) 177.
- [27] A.L. Medina-Castillo, J.F. Fernández-Sánchez, C. Klein, M.K. Nazeeruddin, A. Segura-Carretero, A. Fernández-Gutiérrez, M. Graetzel, U.E. Spichiger-Keller, *Analyst (Cambridge, UK)* 132 (2007) 929.
- [28] C.S.K. Mak, D. Pentlehner, M. Stich, O.S. Wolfbeis, W.K. Chan, H. Yersin, *Chem. Mater.* 21 (2009) 2173.
- [29] Y. Shen, B.P. Maliwal, J.R. Lakowicz, *J. Fluoresc.* 11 (2001) 315.
- [30] Y. Amao, *Microchim. Acta* 143 (2003) 1.
- [31] G. Vicentini, L.B. Zinner, J. Zukerman-Schpector, K. Zinner, *Coord. Chem. Rev.* 196 (2000) 353.
- [32] S.M. Borisov, V.V. Vasil'ev, *J. Anal. Chem.* 59 (2004) 155.
- [33] Y. Amao, Y. Ishikawa, I. Okura, T. Miyashita, *Bull. Chem. Soc. Jpn.* 74 (2001) 2445.
- [34] S. Blair, R. Katakay, D. Parker, *New J. Chem.* 26 (2002) 530.
- [35] Y. Amao, I. Okura, T. Miyashita, *Bull. Chem. Soc. Jpn.* 73 (2000) 2663.
- [36] C.S. Chu, Y.L. Lo, *Sens. Actuators, B* 124 (2007) 376.
- [37] K. Kalyanasundaram, *Photochemistry of Polypyridine and Porphyrin Complexes*, Academic Press, New York, USA, 1992 p. 500.
- [38] Y. Amao, T. Miyashita, I. Okura, *J. Porphyrins Phthalocyanines* 5 (2001) 433.
- [39] C. Huo, H. Zhang, H. Zhang, H. Zhang, B. Yang, P. Zhang, Y. Wang, *Inorg. Chem.* 45 (2006) 4735.
- [40] H. Zhang, Y. Sun, K. Ye, P. Zhang, Y. Wang, *J. Mater. Chem.* 15 (2005) 3181.
- [41] Y. Amao, K. Asai, K. Miyakawa, I. Okura, *J. Porphyrins Phthalocyanines* 4 (2000) 19.
- [42] Y. Kostov, P. Harms, R.S. Pilato, G. Rao, *Analyst (Cambridge, UK)* 125 (2000) 1175.
- [43] H. Hochreiner, I. Sánchez-Barragán, J.M. Costa-Fernández, A. Sanz-Medel, *Talanta* 66 (2005) 611.
- [44] R. Katoh, M. Nakamura, Y. Sasaki, A. Furube, T. Yokoyama, H. Nanjo, *Chem. Lett.* 36 (2007) 1310.
- [45] S. Nagl, C. Baleizão, S.M. Borisov, M. Schäferling, M.N. Berberan-Santos, O.S. Wolfbeis, *Angew. Chem., Int. Ed. Engl.* 46 (2007) 2317.
- [46] Z. Cheng, C.A. Aspinwall, *Analyst (Cambridge, UK)* 131 (2006) 236.
- [47] K.P. McNamara, Z. Rosenzweig, *Anal. Chem.* 70 (1998) 4853.
- [48] J. Ji, N. Rosenzweig, I. Jones, Z. Rosenzweig, *Anal. Chem.* 73 (2001) 3521.
- [49] C. Wu, B. Bull, K. Christensen, J. McNeill, *Angew. Chem., Int. Ed. Engl.* 48 (2009) 2741.
- [50] I.L. Medintz, H.T. Uyeda, E.R. Goldman, H. Mattoussi, *Nat. Mater.* 4 (2005) 435.
- [51] Y. Xia, T. Zhang, X. Diao, C. Zhu, *Chem. Lett.* 36 (2007) 242.
- [52] P.A.S. Jorge, M. Mayeh, R. Benrashid, P. Caldas, J.L. Santos, F. Farahi, *Appl. Opt.* 45 (2006) 3760.
- [53] P.A.S. Jorge, C. Maule, A.J. Silva, R. Benrashid, J.L. Santos, F. Farahi, *Anal. Chim. Acta* 606 (2008) 223.
- [54] S.M. Borisov, A.S. Vasylevska, C. Krause, O.S. Wolfbeis, *Adv. Funct. Mater.* 16 (2006) 1536.
- [55] S.M. Borisov, O.S. Wolfbeis, *Anal. Chem.* 78 (2006) 5094.
- [56] M.I.J. Stich, M. Schaeferling, O.S. Wolfbeis, *Adv. Mater.* 21 (2009) 2216.
- [57] Y. Amao, K. Miyakawa, I. Okura, *J. Mater. Chem.* 10 (2000) 305.
- [58] B.W.K. Chu, V.W.W. Yam, *Langmuir* 22 (2006) 7437.
- [59] Z. Wang, A.R. McWilliams, C.E.B. Evans, X. Lu, S. Chuang, M.A. Winnik, I. Manners, *Adv. Funct. Mater.* 12 (2002) 415.
- [60] D. Avnir, D. Levy, R. Reisfeld, *J. Phys. Chem.* 88 (1984) 5956.
- [61] S.M. Borisov, C. Krause, S. Arain, O.S. Wolfbeis, *Adv. Mater.* 18 (2006) 1511.
- [62] S.M. Borisov, T. Mayr, I. Klimant, *Anal. Chem.* 80 (2008) 573.
- [63] P. Hartmann, M.J.P. Leiner, M.E. Lippitsch, *Anal. Chem.* 67 (1995) 88.
- [64] Y. Amao, K. Asai, T. Miyashita, I. Okura, *Polym. Adv. Technol.* 11 (2000) 705.
- [65] M. Pagliaro, R. Ciriminna, *J. Mater. Chem.* 15 (2005) 4981.
- [66] Y. Amao, Y. Tabuchi, Y. Yamashita, K. Kimura, *Eur. Polym. J.* 38 (2002) 675.
- [67] R. Zusman, C. Rottman, M. Ottolenghi, D. Avnir, *J. Non-Cryst. Solids.* 122 (1990) 107.
- [68] J.D. Mackenzie, E.P. Bescher, *J. Sol-Gel Sci. Tech.* 13 (1998) 371.
- [69] H. Schmidt, G. Jonschker, S. Goedicke, M. Mennig, *J. Sol-Gel Sci. Tech.* 19 (2000) 39.
- [70] C. Sanchez, F. Ribot, B. Lebeau, *J. Mater. Chem.* 9 (1999) 35.
- [71] C. Malins, S. Fanni, H.G. Glever, J.G. Vos, B.D. MacCraith, *Anal. Commun.* 36 (1999) 3.
- [72] A.C. Franville, D. Zambon, R. Mahiou, *Chem. Mater.* 12 (2000) 428.
- [73] L. Cot, A. Ayrat, J. Durand, C. Guizard, N. Hovnanian, A. Julbe, A. Larbot, *Solid State Sci.* 2 (2000) 313.
- [74] A.M. Lazarin, Y. Gushikem, S.C. Castro, *J. Mater. Chem.* 10 (2000) 2526.
- [75] L.R.D. Silva, Y. Gushikem, M.C. Gonçalves, U.P.R. Filho, S.C. Castro, *J. Appl. Polym. Sci.* 58 (1995) 1669.
- [76] U.P.R. Filho, Y. Gushikem, F.Y. Fujiwara, S.C. Castro, I.C.L. Torriani, L.P. Cavalcanti, *Langmuir* 10 (1994) 4357.
- [77] S. Chatterjee, S. Sarkar, S.N. Bhattacharyya, *Polymer* 34 (1993) 1979.
- [78] E.A. Toledo, Y. Gushikem, S.C. Castro, *J. Colloid Interf. Sci.* 225 (2000) 455.
- [79] Q.F. Wang, D.Y. Yu, Y. Wang, J.Q. Sun, J.C. Shen, *Langmuir* 24 (2008) 11684.
- [80] J.F. Fernández-Sánchez, R. Cannas, S. Spichiger, R. Steiger, U.E. Spichiger-Keller, *Anal. Chim. Acta* 566 (2006) 271.

- [81] N.M. Wara, L.F. Francis, B.V. Velamakanni, *J. Membr. Sci.* 104 (1995) 43.
- [82] X. Lu, I. Manners, M.A. Winnik, *Macromolecules* 34 (2001) 1917.
- [83] X. Lu, M.A. Winnik, *Chem. Mater.* 13 (2001) 3449.
- [84] H. Schmidt, *Mat. Res. Soc. Symp. Proc* 32 (1984) 327.
- [85] C. McDonagh, B.D. MacCraith, A.K. McEvoy, *Anal. Chem.* 70 (1998) 45.
- [86] I. Klimant, F. Ruckruh, G. Liebsch, C. Stangelmayer, O.S. Wolfbeis, *Mikrochim Acta* 131 (1999) 35.
- [87] R.M. Bukowski, R. Ciriminna, M. Pagliaro, F.V. Bright, *Anal. Chem.* 77 (2005) 2670.
- [88] R. Camprostrini, M. Ischia, G. Carturan, L. Armelao, *J. Sol-Gel Sci. Technol.* 23 (2002) 107.
- [89] G.R. Atkins, R.B. Charters, *J. Sol-Gel Sci. Technol.* 26 (2003) 919.
- [90] I. Sánchez-Barragán, J.M. Costa-Fernández, M. Valledor, J.C. Campo, A. Sanz-Medel, *Trends Anal. Chem.* 25 (2006) 958.
- [91] J.N. Demas, B.A. DeGraff, P.B. Coleman, *Anal. Chem.* 71 (1999) 793A.
- [92] Y. Kostov, G. Rao, *Sens. Actuators, B* 90 (2003) 139.
- [93] C.S. Chu, Y.L. Lo, *Sens. Actuators, B* 134 (2008) 711.
- [94] K.J. Morris, M.S. Roach, W. Xu, J.N. Demas, B.A. DeGraff, *Anal. Chem.* 79 (2007) 9310.
- [95] M.E. Lippitsch, S. Draxler, D. Kieslinger, *Sens. Actuators, B* 38–39 (1997) 96.
- [96] K.K. Sharman, A. Periasamy, H. Ashworth, J.N. Demas, N. Snow, *Anal. Chem.* 71 (1999) 947.
- [97] G. Liebsch, I. Klimant, C. Krause, O.S. Wolfbeis, *Anal. Chem.* 73 (2001) 4354.
- [98] M. Valledor, J.C. Campo, I. Sánchez-Barragán, J.C. Viera, J.M. Costa-Fernández, A. Sanz-Medel, *Sens. Actuators, B* 117 (2006) 266.
- [99] V.I. Ogurtsov, D.B. Papkovsky, *Sens. Actuators, B* 51 (1998) 377.
- [100] W. Trettnak, C. Kolle, F. Reininger, C. Dolezal, P. O'Leary, *Sens. Actuators, B* 35–36 (1996) 506.
- [101] Y. Kostov, K.A. Van Houten, P. Harms, R.S. Pilato, G. Rao, *Appl. Spectrosc.* 54 (2000) 864.
- [102] M. Valledor, J.C. Campo, F. Ferrero, I. Sánchez-Barragán, J.M. Costa-Fernández, A. Sanz-Medel, *Sens. Actuators, B* 139 (2009) 237.
- [103] J.R. Lakowicz, *Principles of Fluorescence Spectroscopy*, Second edition., Kluwer Academic/Plenum Publishers, New York, USA, 1999 pp. 12–13.
- [104] Y. Kostov, Z. Gryczynski, G. Rao, *Anal. Chem.* 74 (2002) 2167.
- [105] C. Preininger, I. Klimant, O.S. Wolfbeis, *Anal. Chem.* 66 (1994) 1841.
- [106] B.T. Glazer, A.G. Marsh, K. Stierhoff, G.W. Luther, *Anal. Chim. Acta* 518 (2004) 93.
- [107] Y. Amao, T. Miyashita, I. Okura, *Anal. Chim. Acta* 421 (2000) 167.
- [108] J.N. Demas, B.A. DeGraff, *J. Chem. Educ.* 74 (1997) 690.
- [109] K. Mitsubayashi, Y. Wakabayashi, D. Murotomi, T. Yamada, T. Kawase, S. Iwagaki, I. Karube, *Sens. Actuators, B* 95 (2003) 373.
- [110] R.C. Evans, P. Douglas, J.A.G. Williams, D.L. Rochester, *J. Fluoresc.* 16 (2006) 201.
- [111] R.C. Evans, P. Douglas, *Anal. Chem.* 78 (2006) 5645.
- [112] R.C. Evans, P. Douglas, *ACS Appl. Mater. Interfaces* 1 (2009) 1023.
- [113] S.R. Ricketts, P. Douglas, *Sens. Actuators, B* 135 (2008) 46.
- [114] X.D. Wang, X. Chen, Z.X. Xie, X.R. Wang, *Angew. Chem., Int. Ed. Engl.* 47 (2008) 7450.
- [115] P. Jorge, C. Maule, A. Silva, R. Benrashid, J. Santos, F. Farahi, *Anal. Chim. Acta* 606 (2008) 223.
- [116] R.W.T. Higgins, A.P. Monkman, *J. Appl. Phys.* 91 (2002) 99.
- [117] C.M. Che, Y.J. Hou, M.C.W. Chan, J. Guo, Y. Liu, Y. Wang, *J. Mater. Chem.* 13 (2003) 1362.